



Published in final edited form as:

Neuroimage. 2007 March ; 35(1): 140–148.

Cortical Abnormalities in Epilepsy Revealed by Local EEG Synchrony

C. Schevon^b, J. Cappell^{b,c}, R. Emerson^{b,c}, J. Isler^c, P. Grieve^c, R. Goodman^d, G. Mckhann jr^d, H. Weiner^e, W. Doyle^{a,e}, R. Kuzniecky^a, O. Devinsky^a, and F. Gilliam^b

b Department of Neurology, Columbia University Medical Center, NY

c Department of Pediatrics, Columbia University Medical Center, NY

d Department of Neurosurgery, Columbia University Medical Center, NY

a Department of Neurology, NYU Medical Center

e Department of Neurosurgery, NYU Medical Center

Abstract

Abnormally strong functional linkage between cortical areas has been postulated to play a role in the pathogenesis of partial epilepsy. We explore the possibility that such linkages may be manifest in the interictal EEG apart from epileptiform disturbances or visually evident focal abnormalities. We analyzed samples of interictal intracranial EEG (ICEEG) recorded from subdural grids in nine patients with medically intractable partial epilepsy, measuring interelectrode synchrony using the mean phase coherence algorithm. This analysis revealed areas of elevated local synchrony, or “hypersynchrony” which had persistent spatiotemporal characteristics that were unique to each patient. Measuring local synchrony in a subdural grid results in a map of the cortical surface that provides information not visually apparent on either EEG or structural imaging. We explore the relationship of hypersynchronous areas to the clinical evidence of seizure localization in each case, and speculate that local hypersynchrony may be a marker of epileptogenic cortex, and may prove to be a valuable aid to clinical ICEEG interpretation.

Keywords

Epilepsy surgery; synchrony; intracranial EEG; epileptogenic zone; seizure localization

Introduction

Resective epilepsy surgery for refractory seizures targets the epileptogenic zone, the minimum region of cortex whose removal is both necessary and sufficient to abolish seizures (Luders and Awad 1991; Engel 2003). Analysis of intracranial EEG (ICEEG) ictal recordings to identify the epileptogenic zone is generally more specific than information provided by seizure semiology, neuroimaging or neuropsychological testing (Engel, Henry et al. 1990). Visual interpretation of the intracranial EEG (ICEEG) is a clinically reliable tool for identifying the

Corresponding author: Catherine Schevon, M.D., Ph.D. Neurological Institute of New York, 710 West 168th Street, 7th floor, New York, NY 10032, Phone: (212) 305-2121, Fax: (212) 305-5445, Email: cas2044@columbia.edu

Financial interests: This work was supported by NINDS grants 1 K08 NS48871 R1A1 and 5 K12 NS001698.

Publisher's Disclaimer: This is a PDF file of an unedited manuscript that has been accepted for publication. As a service to our customers we are providing this early version of the manuscript. The manuscript will undergo copyediting, typesetting, and review of the resulting proof before it is published in its final citable form. Please note that during the production process errors may be discovered which could affect the content, and all legal disclaimers that apply to the journal pertain.

epileptogenic zone in mesial temporal epilepsy (Pacia and Ebersole 1999) but has more variable success in predicting surgical control of neocortical seizures, particularly in cases where neuroimaging does not show focal abnormalities (Alarcon, Binnie et al. 1995; Ebersole 1999; Jung, Pacia et al. 1999).

While the interpretation of the ICEEG has traditionally been oriented toward paroxysmal epileptiform disturbances of cerebral activity, it is known that persistent non-epileptiform background abnormalities, for example focal delta range activity, are characteristic of dysfunctional cortical regions. Paroxysmal epileptiform discharges are thought to be more specific for epileptogenicity. Extending interictal ICEEG interpretation using quantitative techniques, however, have disclosed critical background features relevant to surgical decision-making that are not apparent to visual inspection. For example, very high frequency (> 100 Hz), low amplitude activity ($< 5 \mu\text{V}$) has been associated with the epileptogenic zone (Worrell, Parish et al. 2004; Alarcon, Binnie et al. 1995; Allen, Fish et al. 1992), as has neuronal synchrony recorded from hippocampal microelectrodes (Colder, Wilson et al. 1996) and spectrogram measurements of EEG amplitude (Asano, Muzik et al. 2004). Such techniques may be used to detect signatures of cortical abnormality that are not necessarily associated with the well known paroxysmal features, and that may be linked to seizures. Markers of abnormal tissue have the advantage that they may be more persistent and therefore more reliably detectable than paroxysmal features. To be useful in epilepsy surgical evaluations, such markers would be based on EEG features which closely relate to epileptogenic potential rather than being nonspecific correlates of dysfunction, as well as having a wide diagnostic index; i.e. areas of abnormality should be consistently and markedly different from normal.

We hypothesize that enhanced local synchrony detected in ICEEG recordings may be a marker of epileptogenicity, reflecting abnormal functional connectivity within epileptogenic cortex. A mathematical model of a cortical neuronal network provides support for the view that greater connectivity *per se* among neurons, without alteration of individual firing thresholds, may be sufficient to confer an epileptogenic state (Traub, Whittington et al. 2001). Accordingly, abnormally enhanced synchrony may be expected to be apparent in the background EEG, apart from spike discharges, as it reflects a fundamental property of the underlying cortex. Indeed, coherence, a normalized frequency-dependent measure of correlation, has been shown to be increased over tumors and regions thought to be part of the epileptogenic zone (Towle, Syed et al. 1998; Towle, Carder et al. 1999; Zaveri, Williams et al. 1999). Similarly, changes in phase synchrony, a related measure that has been used to detect EEG changes before seizure onset, also appear to be most prominent proximate to the epileptogenic zone (Lehnertz and Elger 1995; Le Van Quyen, Martinerie et al. 2001; Chavez, Le Van Quyen et al. 2003; Mormann, Andrzejak et al. 2003; Le Van Quyen, Soss et al. 2005).

We report an investigation into spatial patterns of local synchrony in epilepsy patients with medically refractory partial epilepsy using a measure of phase coherence in wide-band ICEEG signals (Mormann, Lehnertz et al. 2000). Based on synchrony measurements of the EEG signals recorded from orthogonally adjacent pairs of electrodes in subdural grids, we are able to define regions of *local hypersynchrony* (LH) in which there are markedly higher levels of synchrony compared to surrounding brain regions. Although the primary goal of this paper is to define the properties of these hypersynchronous regions, we also investigate a possible correlation with the epileptogenic zone. Cortical landmarks that may have the LH property include structural abnormalities identified on neuroimaging that have given rise to seizures, areas in which active paroxysmal activity is present, and areas adjacent to ictal onset zones.

Methods

Data were collected from patients undergoing ICEEG monitoring prior to resective surgery at Columbia University and New York University Medical Centers. IRB approval for the retrospective analysis of clinical data was obtained at both institutions. Arrays of platinum electrodes, 5 mm in diameter with 10 mm center-to-center spacing (AdTech), were implanted subdurally at sites determined clinically to be likely to encompass the seizure onset zone. Data were sampled at 250 Hz / channel and bandpass filtered between 0.1 – 54 Hz (Xltek, Inc, at Columbia) or 400 Hz / channel, and bandpass filtered from 0.5 – 65 Hz (Nicolet Biomedical, at NYU). For each patient, the epileptogenic zone was defined by at least two treating epileptologists based on visual interpretation of the ICEEG (both seizure onset and interictal localization) and other available clinical data. Surgical resection was based on clinical criteria, including neuroimaging findings, interpretation of the ICEEG, and location of eloquent cortex defined by functional mapping. The results of the quantitative analysis (described below) were not included in the decision-making process.

Quantitative analysis was performed on selected interictal samples. For eight patients, three 5-minute interictal EEG samples, selected to be free of artifact and recorded not less than six hours before or after a seizure, were used for analysis. For one patient (Patient 2), the analysis was performed on selected time samples over 5 days of consecutive EEG; the recording was inspected visually, and segments containing recognizable artifact were excluded. Samples were chosen to exclude interictal epileptiform discharges to the extent possible. Post-implant MRIs were available for seven patients (Patients 3 through 9); from these, 3 dimensional MRI reconstruction of the cortical surface, indicating estimated electrode positions, were created using MRIcro (C. Rorden, University of South Carolina).

Interelectrode synchrony was measured using the mean phase coherence (MPC) algorithm (Mormann, Lehnertz et al. 2000) and implemented in Matlab. This algorithm measures phase locking of broad-band EEG signals from two electrodes independent of their predominant phase angles. As such, it is unaffected by constant phase delay between the signals, as, for example, would be produced by neural transmission time between distant recording sites. Further, MPC reflects phase independent of amplitude. Since the amplitude of EEG signals recorded from subdural electrodes may be influenced by mechanical factors such as the precise relationship of the electrode to the brain surface, amplitude independence increases the robustness of the measure.

Mean phase coherence is computed by first applying the Hilbert transform to a pair of input signals to obtain the instantaneous phase values. These are then projected onto the unit circle and the distance between them is measured using a trigonometric conversion of angular distance, producing a measure of the normalized total coherence between the predominant phase present in each of the two signals:

$$\left| \text{MPC} = \frac{1}{N} \sum_{j=0}^{n-1} e^{i\phi(j/r)} \right|_{\text{fix}}$$

where ϕ represents the instantaneous phase angle and n is the number of input samples. This expression is then converted to a form suitable for computation using Euler's formula, a common trigonometric identity. Note that this method is able to recognize phase differences that cross the zero line, e.g. 10 degrees and 350 degrees are 20 degrees apart, not 340.

The EEG signals were de-meant and average referenced to minimize distortions created by noise in the standard reference signal, as this can cause spurious decreases in the MPC value (Guevara, Velazquez et al. 2005). Non-recording or noisy channels were eliminated. A

symmetric Chebyshev notch filter was applied to remove electrical (60 Hz) artifact and its harmonics. Pairwise broad-band synchrony was calculated for all grid channels in two-second time epochs with a one second overlap.

This study focuses largely on measurements of *local* synchrony, defined for our purposes as synchrony between adjacent electrodes (one cm apart center-to-center) in a subdural array. Only orthogonally adjacent pairs were used in order to limit comparisons of synchrony to signals recorded at fixed distances. For a given subdural grid recording, the set of local MPC values determines a topographical surface map illustrating spatial variations in local synchrony. To construct the maps, 5 minutes of MPC data was averaged and the interpolated mean phase coherence for the cortical surface under the grid was depicted graphically using the red-blue pseudocolor spectrum. Vertices were assigned to the center points of the edges connecting each channel pair. The Delaunay triangulation, which has the property that all triangles are non-intersecting, was used to generate an interpolated surface plot based on the MPC values of the vertices. All computations were performed using Matlab (Mathworks, Natick, MA).

Electrode pairs for which the 5 minute averaged MPC are significantly higher than expected are designated as *hypersynchronous*. As will be seen, the electrode pair MPC values in our patients did not conform to a unimodal normal distribution, but rather had a prominent positive skew. This finding may be explained by a bimodal Gaussian distribution consisting of electrode pairs that are either normally synchronous or hypersynchronous. Figure 1 illustrates the distribution of local MPC values in the subdural grid recording of Patient 3, with the corresponding probability density functions for both the normally synchronous and hypersynchronous groups. A linear discriminator dividing electrode pairs into the two groups was established by first eliminating the minimum number of high MPC values pairs such that the distribution of MPC value for the remaining pairs were symmetric about the mean, i.e. had zero skew; this represents the Gaussian distribution of the normally synchronous pairs. The MPC threshold value for hypersynchronous electrode pairs was then set to the mean plus twice the standard deviation of this “de-skewed” distribution, represented by the dashed vertical line in Figure 1. This method effectively identifies the hypersynchronous electrode pairs while minimizing the number of incorrectly classified normally synchronous pairs. We refer to these pairs as *locally hypersynchronous* (LH), and to the cortical region outlined by a contiguous set of two or more LH electrode pairs as a *region of local hypersynchrony*.

The identified LH electrode pairs were grouped, where appropriate, into *LH regions*, defined as the cortical surface underlying electrodes included in a set of two or more contiguous LH pairs. These regions were then compared to the resections performed in each case to determine if they were included in the resected tissue. The locations of the resection areas relative to the subdural grids were determined from surgical records and intra-operative photographs. Statistical significance in seizure outcomes between those patients in whom all LH regions were resected vs. those in whom LH regions were not resected were compared using a chi-square test.

Results

Nine patients were studied (9 – 54 years, mean 31 years). Epilepsy duration ranged from one month to 42 years (mean 18.8 years). The location of the subdural grids, associated pathology, the locations of the resections and LH regions, and surgical outcome are summarized in Table 1. Overall, the surgical resection included all locally hypersynchronous areas in two patients (5 and 6) and did not include all such regions in six patients (1, 2, 3, 7, 8 and 9). Seizure outcome following surgery was assessed as “no change”, “improved”, and “seizure free”, with follow-up period ranging from 6 months to 2 years. Data were not available for one patient (4).

Two patients (4 and 5) had well-defined structural lesions in the temporal lobe (cavernous angioma, low-grade glioma). One had cortical dysplasia in the left perisylvian region (Patient 2); resection of the epileptogenic zone was limited by the presence of eloquent cortex. Two more had nondominant mesial temporal lobe epilepsy with clinical evidence of an additional extratemporal focus (Patients 6 and 7). While both underwent standard non-dominant temporal lobectomy following implantation, Patient 6 had an additional parietal topectomy due to a small focus of interictal epileptiform activity. One patient (3) had inflammatory changes in the left perisylvian region secondary to Parry-Romberg syndrome of progressive facial hemiatrophy and medically refractory simple partial status epilepticus (for a recent review, see (Paprocka, Jamroz et al. 2005)). Multistage surgery was performed for control of refractory complex partial status epilepticus, with an anterior temporal resection during the second surgical stage and a frontal opercular resection or deafferentation in the third stage. The remaining patients (1, 8, and 9) were nonlesional extratemporal cases, with no conclusive pathological diagnosis following resection. Both of these patients underwent partial frontal lobectomy, and Patient 9 had additional resection of the anterior temporal lobe.

Statistical and Spatial Characteristics of Local Hypersynchrony

Mean and standard deviation of the local MPC values, separated into LH and non-LH pairs, are shown in Table 2. The distribution of local MPC values in each patient demonstrated a positive skew (Table 2), indicating a preponderance of channel pairs in the tail at the high-valued end (Figure 1). Kurtosis, a measurement indicating the relative number of MPC values located in the tails of the distribution, did not reveal a consistent pattern.

In each patient, one or more LH regions ranging from 2 to 5 cm in maximal diameter were identified. With a single exception, LH regions were well demarcated by an abrupt drop in local synchrony at their edges (Figures 2a, 4, 5a,b,c). Patient 9, who had frontal lobe epilepsy, showed a diffuse pattern of local hypersynchrony in the frontal lobe but interestingly two additional distinct, well demarcated LH regions in parietal and temporal lobes (Figure 5c).

Stability of Local Synchrony

LH regions were stable, constant features of the ICEEG. Figure 2b illustrates the MPC values for all epochs over a 38 minute period for the two noncontiguous LH regions detected in Patient 1 (Figure 2a), compared to the average MPC values computed simultaneously over the entire grid. Despite continuous fluctuations in the MPC values, those in the LH regions remain persistently elevated compared to the grid average.

The MPC measure also appears to maintain stability over longer time periods. We investigated this in Patient 2 by testing artifact-free epochs sampled at regular intervals (approximately every 60 minutes) over a 5 day period, for a total of 125 samples. We found that the 5-minute MPC averages for local channel pairs exhibited generally small variations over time, with a mean percentage deviation from baseline of 6% and standard deviation 2%. Despite these variations, the identity of the LH regions remained largely stable, with some variation occurring at the edges of the regions. Figure 3 shows daily local synchrony “snapshots” of the grid. Note that there are two LH regions, one in on the left side of the grid and the other on the right, that vary somewhat in dimension across the samples. In one snapshot (day 4), the two regions appear connected. To summarize the changes over the 5 day period, an LH “density” map is shown (Figure 3). This map is representative of the 8×8 grid, with the value of each electrode location equal to the percentage of time samples in which that electrode was a member of an LH channel pair. Electrodes consistently identified as LH are concentrated in the two LH regions described, while electrodes that have a variable classification are located along the borders of the regions and the isthmus connecting the two. A similar result was obtained with the EEG samples tested in the other eight patients. Thus, by our definition, the LH property

appears to be sufficiently robust that a single 5 minute interictal EEG sample is capable of providing a reasonable estimate of the LH regions.

Stability of MPC for all patients was established by computing the 5-minute average for three separate interictal data segments, each recorded on a different monitoring day. The results of the comparison of the deviation of the second two samples from the first (baseline) sample are detailed in Table 2. Consistent with our findings in Patient 2, local synchrony values remained relatively stable in each case, with a mean variation of 14% or less (Table 2).

Patient specificity of local hypersynchrony

Anatomical locations and distribution of LH regions appeared patient-specific and did not necessarily conform to natural boundaries such as sulci and major fissures. Although the areas of subdural grid coverage was determined clinically and therefore varied between patients, in seven patients (Patients 1–4, 6, 7, and 9) there were large areas of common coverage including the inferior central and perisylvian regions. Nonetheless, local synchrony patterns in these areas were dissimilar (Figures 2a, 4, and 5). In patients 1, 2, 3, and 6 (Figures 2, 4 and 5b) LH regions encompassed channel pairs that clearly spanned multiple gyri; this argues against the possibility that local synchrony is an artifact of recording from closely-related anatomically connected structures.

Correlation of LH resection to seizure outcome

Two patients (5 and 6) became seizure free following surgery; in both cases, all detected LH regions were resected. The remaining six patients for whom data were available had resections that did not include all identified LH regions. Four showed significant clinical improvement, while Patients 1 and 2 experienced no change in their seizures following resection. In patient 3, intracranial EEG recordings demonstrated widely distributed waxing and waning ictal activity maximal over both left anterior temporal and inferior frontal regions. However, the LH property was largely confined to the inferior frontal (suprasylvian) area (Figure 4). Seizure activity was unaffected by anterior temporal resection, performed in the second surgical stage. Status epilepticus resolved following insular resection and frontal opercular resection or deafferentation in the third surgical stage which included a portion of the major LH area, although occasional seizures continued. Patient 7, while free of seizures with impairment of consciousness after standard nondominant temporal resection, developed a new type of simple partial seizure (facial tingling) consistent with extratemporal origin.

A chi-square comparison was performed between patients who were seizure free after surgery and patients who showed no postoperative improvement, demonstrating that complete LH resection improves clinical outcome ($p < 0.05$). When partial remissions were included, this trend was still apparent although the comparison did not reach statistical significance. This is most likely due to insufficient power given a three-way comparison.

Correlation of LH regions with the epileptogenic zone

In patients in whom the epileptogenic zone (as determined by clinical assessment of the interictal epileptiform activity and ictal onset) was recorded by the subdural grid, there was a recognizable association with LH regions. Generally, the LH regions did not coincide precisely with the clinically determined epileptogenic zone but rather were located in adjacent cortex. This is especially clear in the grid maps for patients 1, 2, 4, 6 and 8. In cases in which there were two or more distinct LH regions, these sometimes bracketed the epileptogenic zone. This is well demonstrated by the data from Patient 8 showing two noncontiguous epileptogenic zones with LH regions both adjacent to and between these zones (Figure 5c).

In both patients (Patients 4 and 5) with structural cortical lesions, an LH region covered part of the lesion and also an area of adjacent cortex. These extra-lesional areas corresponded to the location of the most prominent interictal activity (Figure 5a). Of note, patient 4, who had long standing seizures due to a temporal cavernous angioma, also exhibited additional distant frontal LH regions; one of these was also associated with frequent interictal discharges.

Two patients (6 and 7) with mesial temporal plus parietal lobe seizure foci (the “dual pathology” syndrome) exhibited small, well defined regions of hypersynchrony in the parietal lobe (Figure 5b). Patient 6, who had frequent typical mesial temporal onset seizures as well as rare seizures preceded by arm tingling, demonstrated focal parietal interictal spiking and coincident LH. Patient 7 demonstrated an LH region immediately posterior to an area of mixed face and hand function identified on extraoperative stimulation mapping, however the clinical EEG interpretation revealed no other extratemporal EEG abnormalities. Anteromesial temporal lobe resection resolved this patient’s habitual complex partial seizures, but a new seizure type developed characterized by contralateral facial tingling.

Patients 8 and 9 with non-lesional frontal lobe epilepsy syndromes showed more complex patterns of local hypersynchrony. In Patient 9, LH regions were distributed widely in the frontal lobe. Interestingly, additional LH regions were noted at restricted sites in temporal and parietal lobes (Figure 5c). The EEG showed broadly distributed interictal activity and seizure onsets that were diffuse, but maximal in regions corresponding to the LH areas. This patient had multiple daily tonic seizures prior to surgery, and became nearly seizure free during six months of follow-up after resection that included the frontal and anterior temporal LH regions. No parietal resection was performed as the epileptogenic region in this lobe was found to contain language-critical function.

Long range synchronization between LH regions

Long range synchronization between LH regions was evaluated in Patients 1, 6, and 9. The data for Patient 1, shown in Figure 6, revealed that the mean phase coherence (averaged over the set of electrode pairs the same distance apart) generally has an inverse exponential relationship with distance when both electrodes in a pair are outside LH areas (dots). However, for a given distance, synchrony was nearly always greater when both electrodes were within an LH region (squares) and in pairs spanning non-contiguous LH regions (crosses). In this case, synchrony between noncontiguous LH regions was markedly more prominent than that within LH regions. A similar pattern of increased long distance synchrony between LH regions was seen in Patient 9, although the inter-region and within-region synchrony values were not dissimilar. The finding, however, was not universal, as Patient 6 did not demonstrate the strong coupling between distant electrodes located in LH regions.

Discussion

Mean phase coherence calculated on orthogonally adjacent electrode pairs provides spatial and temporal information about phase locking of local field potentials at neighboring sites in the neocortex. The distribution of the obtained measurements is characterized by a consistent positive skew, and may be explained by two sets of normally distributed values with differing means. Similar observations have been made for measurements of coherence in ECoG recordings (Towle, Syed et al. 1998). Our findings indicate that regions of locally enhanced synchronized neuronal activity exist in patients with epilepsy. These findings are consistent with earlier reports of localized synchrony measurements in human epilepsy patients (Le Van Quyen, Soss et al. 2005) and a cat model of seizures (Valentine, Teskey et al. 2004). LH regions appear to be stable, i.e. mean phase coherence remains consistently elevated, when measured for periods of up to several days. As such, it appears that LH may be a fundamental property of the underlying cortex. Further, these regions appear to be patient-specific; we speculate that

the mechanisms determining local hypersynchrony may be related to the abnormalities that underlie partial epilepsy.

These findings suggest that local hypersynchrony is unlikely to be a normal phenomenon. We did not directly assess MPC in normals, and indeed its direct measurement may be difficult in intact humans because LH regions are often too small (2 – 5 cm in our patients) to be detectable on scalp surface recordings. A study of local and distant synchrony in MEG recordings of patients with generalized epilepsy and normal controls did not reveal significant spatial heterogeneity in either group (Dominguez, Wennberg et. al., 2005). Although it would have been difficult to detect small hypersynchronous regions in their study, it suggests that local hypersynchrony is not a ubiquitous phenomenon in the studied populations. In the present study, in which a portion of the cortical surface was examined, local hypersynchrony were detected in each case. In patients with focal lesions the LH regions appeared to overlap the pathological features (Table 1; Patient 2, 4 and 5), although in Patients 4 and 5, not all of the electrodes over the structural lesions displayed the hypersynchrony property (Figure 5a). Thus, it appears that local hypersynchrony, while probably abnormal, is not necessarily a direct consequence of cortical damage.

Spatial patterns of local hypersynchrony appeared to be unique to each patient studied; no specific areas were hypersynchronous in all patients tested despite considerable overlap in the anatomic regions surveyed by the implanted grids. In those patients in whom the epileptogenic zone was covered by the subdural grid, there appeared to be an association between the epileptogenic zone and LH regions, however they were more likely to be adjacent than concordant, as demonstrated by Patients 1, 2, 4, 6, and 8. These findings are consistent with prior observations of elevated local coherence over tumors and epileptogenic areas observed during intraoperative corticography (Towle, Syed et al.; Towle, Carder et al. 1999), wavelet-based synchrony in chronic ICEEG recordings of a patient with a large frontal tumor (Le Van Quyen, Soss et al. 2005) and cross correlation of microelectrode recordings using a non-lesional cat model of seizures (Valentine, Teskey et al. 2004). In the cases in which there was concordance between the epileptogenic zone and an LH region (Patients 5, 6, and 9), the epileptogenic zone (or the portion that was recorded from the subdural grid) was determined primarily from interictal activity rather than from seizure onsets. While this suggests that local hypersynchrony may be a reflection primarily of interictal activity, we have found that in general, LH is located over a more restricted area than is the case with interictal activity. This phenomenon is well demonstrated in Patient 9 (Figure 5c). Additionally, LH regions have been found in areas in which no interictal abnormalities were observed, as was seen in Patient 7 (Figure 5b).

Based on the small number of cases presented here, we speculate that resection of LH regions may contribute to surgical control of seizures. The inferential analysis performed included in this study suggests that this may be the case. However, it must be recognized that conclusions drawn from these results are limited due to the fact that only subdural grid recordings were analyzed, thus limiting the analysis to those cortical regions covered by the grids.

The correlation of complete resection of LH regions with good surgical outcome and the spatial association of LH regions with the clinically determined epileptogenic zone suggests that the LH regions are markers of epileptogenic cortex rather than nonspecific indicators of cortical dysfunction. In nonlesional epilepsy, such dysfunction would be expected to derive primarily from localized reorganization within the epileptogenic zone and repeated potentiation of seizure propagation pathways, which may extend beyond the source of epileptogenic activity. It remains to be seen whether the LH property is capable of distinguishing these types of abnormalities. If so, this phenomenon may be unique in that it is a persistent interictal feature that provides specific information about the epileptogenic zone. However, establishing the true

etiology of local hypersynchrony will require more detailed study and larger sample sizes than that presented here.

The theory that epileptogenic networks contribute to the generation of partial seizures has been advanced by multiple authors (Bragin, Wilson et al. 2000;Spencer 2002). These networks are postulated to consist of local clusters of neurons distributed in multiple locations, possibly in multiple lobes (Colder et al., 1996;Bragin, Wilson et al. 2000 Bartolomei et al., 2001). This construction implies both increased long range synchrony between clusters, as well as increased local communication within clusters. These are the specific attributes which we have observed in LH areas, although there appeared to be some variation in distant synchrony measurements between patients. Accordingly, we speculate that when multiple regions of mutually synchronous LH regions exist, they may identify the location and structure of an individual patient's epileptogenic network. Additionally, the variation seen in the long distance synchrony measurements between noncontiguous LH regions may have implications for their participation in epileptogenic networks. For example, Patient 9's map suggests a large tri-lobar network. Although this patient's surgery was intended to be palliative due to poorly localized seizures, a surprising degree of success was achieved when two of the three LH regions were resected. It is possible that disconnection rather than complete removal of the separate nodes of the epileptogenic network is sufficient to disable the process of seizure generation.

The ability to characterize an individual's epilepsy syndrome not only by the location of a specific seizure onset zone but by the anatomical distribution and functional interrelationships of the epileptogenic network may lead to improvements in surgical approaches and outcomes. Further, it is attractive to speculate that in order to prevent seizures, it may be necessary to identify and either remove or disconnect key nodes of the network. In this view, the epileptogenic zone becomes synonymous with the location of nodes of the epileptogenic network; these may be either focal or widely distributed. As such, an important direction in epilepsy surgery will be the Identification of these nodes via highly granular electrophysiology recordings along with enhanced analysis capable of revealing functional relationships between neuronal ensembles.

References

- Alarcon G, Binnie CD, et al. Power spectrum and intracranial EEG patterns at seizure onset in partial epilepsy. *Electroencephalogr Clin Neurophysiol* 1995;94:326–337. [PubMed: 7774519]
- Allen PJ, Fish DR, et al. Very high-frequency rhythmic activity during SEEG suppression in frontal lobe epilepsy. *Electroencephalography and Clinical Neurophysiology* 1992;82(2):155–59. [PubMed: 1370786]
- Asano E, Muzik O, et al. Quantitative visualization of ictal subdural EEG changes in children with neocortical focal seizures. *Clinical Neurophysiology* 2004;115(12):2718–27. [PubMed: 15546780]
- Blumenfeld H. Positive and negative network correlations in temporal lobe epilepsy.
- Bragin A, Wilson CL, et al. Chronic epileptogenesis requires development of a network of pathologically interconnected neuron clusters: a hypothesis. *Epilepsia* 2000;41(Suppl 6):S144–52. [PubMed: 10999536]
- Bartolomei F, Wendling F, et al. Neural networks involving the medial temporal structures in temporal lobe epilepsy. *Clin Neurophys* 2001;112(9):1746–60.
- Chavez M, Le Van Quyen M, et al. Spatio-temporal dynamic prior to neocortical seizures: amplitude vs. phase couplings. *IEEE Transactions on Biomedical Engineering* 2003;50(5):571–83. [PubMed: 12769433]
- Colder BW, Wilson CL, et al. Neuronal synchrony in relation to burst discharge in epileptic human temporal lobes. *J Neurophysiol* 1996;75(6):2496–508. [PubMed: 8793759]

- Dominguez LG, Wennberg R, et al. Enhanced synchrony in epileptiform activity? Local versus distant phase synchronization in generalized seizures. *Journal of Neuroscience* 2005;25(35):8077–84. [PubMed: 16135765]
- Ebersole JS. Intracranial EEG: the last word. *Journal of Clinical Neurophysiology* 1999;16(5):495–7. [PubMed: 10576232]
- Engel J. Practice parameter: temporal lobe and localized neocortical resections for epilepsy. *Epilepsia* 2003;44(6)
- Engel J, Henry TR, et al. Presurgical evaluation for partial epilepsy: relative contributions of chronic depth-electrode recordings versus FDG-PET and scalp-sphenoidal ictal EEG. *Neurology* 1990;40(11)
- Guevara R, Velazquez JL, et al. Phase synchronization measurements using electroencephalographic recordings: what can we really say about neuronal synchrony? *Neuroinformatics* 2005;3(4):301–14. [PubMed: 16284413]
- Jung WY, Pacia SV, et al. Neocortical temporal lobe epilepsy: intracranial EEG features and surgical outcome. *Journal of Clinical Neurophysiology* 1999;16(5):419–25. [PubMed: 10576224]
- Le Van Quyen M, Martinerie J, et al. Characterizing neurodynamic changes before seizures. *Journal of Clinical Neurophysiology* 2001;18(3):191–208. [PubMed: 11528293]
- Le Van Quyen M, Soss J, et al. Preictal state identification by synchronization changes in long-term intracranial EEG recordings. *Clinical Neurophysiology* 2005;116(3):559–68. [PubMed: 15721070]
- Lehnertz K, Elger CE. Spatio-temporal dynamics of the primary epileptogenic area in temporal lobe epilepsy characterized by neuronal complexity loss. *Electroencephalogr Clin Neurophysiol* 1995;95:108–117. [PubMed: 7649002]
- Luders, HO.; Awad, I. Conceptual considerations. In: Luders, HO., editor. *Epilepsy Surgery*. New York: Raven Press; 1991.
- Mormann F, Andrzejak RG, et al. Automated detection of a pre-seizure state based on a decrease in synchronization in intracranial electroencephalogram recordings from epilepsy patients. *Phys Rev E Stat Nonlin Soft Matter Phys* 2003;67(2 Pt 1)
- Mormann F, Lehnertz K, et al. Mean phase coherence as a measure for phase synchronization and its application to the EEG of epilepsy patients. *Physica D* 2000;144:358–369.
- Pacia SV, Ebersole JS. Intracranial EEG in temporal lobe epilepsy. *Journal of Clinical Neurophysiology* 1999;16(5):399–407. [PubMed: 10576222]
- Paprocka J, Jamroz E, et al. Difficulties in differentiation of Parry-Romberg syndrome, unilateral facial scleroderma, and Rasmussen syndrome. *Childs Nerv Syst*. 2005
- Quesney, LF.; Constain, M., et al. How large are frontal lobe zones? EEG, EcoG, and SEEG evidence. In: Chauvel, P.; Delgado-Escueta, AV.; Halgren, E., editors. *Advances in neurology: frontal lobe seizures and epilepsies*. New York: Raven Press; 1992. p. 311-23.
- Spencer SS. Neural Networks in Human Epilepsy: Evidence of and Implications for Treatment. *Epilepsia* 2002;43(3):219–227. [PubMed: 11906505]
- Towle VL, Carder RK, et al. Electroencephalographic coherence patterns. *Journal of Clinical Neurophysiology* 1999;16(6):528–47. [PubMed: 10600021]
- Towle VL, Syed I, et al. Identification of the sensory/motor area and pathological regions using ECoG coherence. *Electroencephalogr Clin Neurophysiol* 1998;106(1):30–9. [PubMed: 9680162]
- Traub RD, Whittington MA, et al. A Possible Role for Gap Junctions in Generation of Very Fast EEG Oscillations Preceding the Onset of, and Perhaps Initiating, Seizures. *Epilepsia* 2001;42(2):153–170. [PubMed: 11240585]
- Valentine PA, Teskey GC, et al. Kindling changes burst firing, neural synchrony, and tonotopic organization of cat primary auditory cortex. *Cerebral Cortex* 2004;14(8):827–39. [PubMed: 15054056]
- Worrell GA, Parish L, et al. High-frequency oscillations and seizure generation in neocortical epilepsy. *Brain* 2004;127(7):1496–1506. [PubMed: 15155522]
- Zaveri HP, Williams WJ, et al. Measuring the coherence of intracranial electroencephalograms. *Clinical Neurophysiology* 1999;110:1717–25. [PubMed: 10574287]

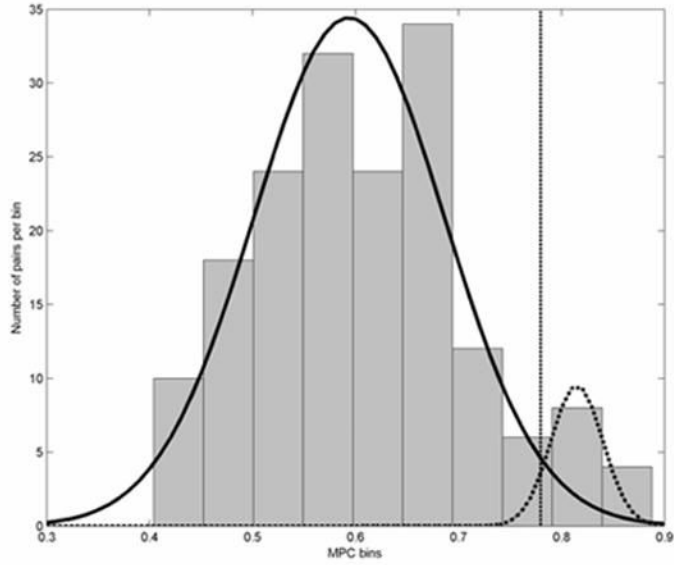


Figure 1. Histogram of MPC values and probability density functions showing the bimodal Gaussian distribution of non-LH (solid density curve, left) and LH (dotted curve, right) electrode pairs. Probability density curves were calculated from the mean and standard deviations of the MPC values in the two groups of electrode pairs. The linear discriminator dividing the two groups is shown as a dashed vertical line. These data are from Patient 3's subdural grid.

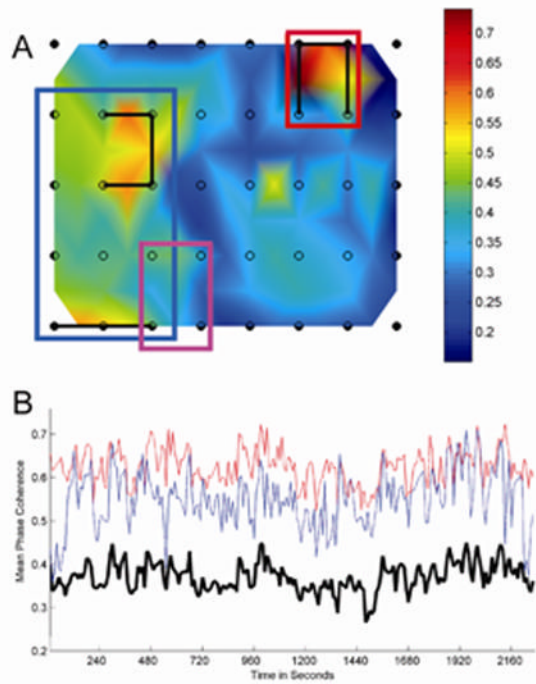


Figure 2.

Patient 1, with nonlesional neocortical epilepsy and an 8×5 subdural grid placed over the right posterior temporal/central region. Grid location was determined by visual observation at time of implantation and confirmed by postoperative radiograph. a) Surface map of the 8×5 subdural grid depicting 5-minute averaged MPC measures for orthogonally adjacent grid channels. The MPC measure is depicted by a red-blue color map; a sidebar shows the color mapping for each plot. Two major noncontiguous LH regions are present, shown bounded by blue and red rectangles, located in the posterior temporal/occipital region and suprasylvian frontal regions. The clinically determined seizure onset zone is shown for comparison (magenta rectangle). Electrode pairs meeting criteria for local hypersynchrony are marked by connecting black lines. b) Local synchrony, computed over 2 second epochs for a continuous 38 minute interictal recording. The average MPC for the sets of LH channel pairs in each region are averaged and plotted in blue (posterior temporal region) and red (suprasylvian frontal region). Compare with the averaged MPC for all channel pairs (heavy black). Note that the relative values of the LH regions remain persistently high compared to the average.

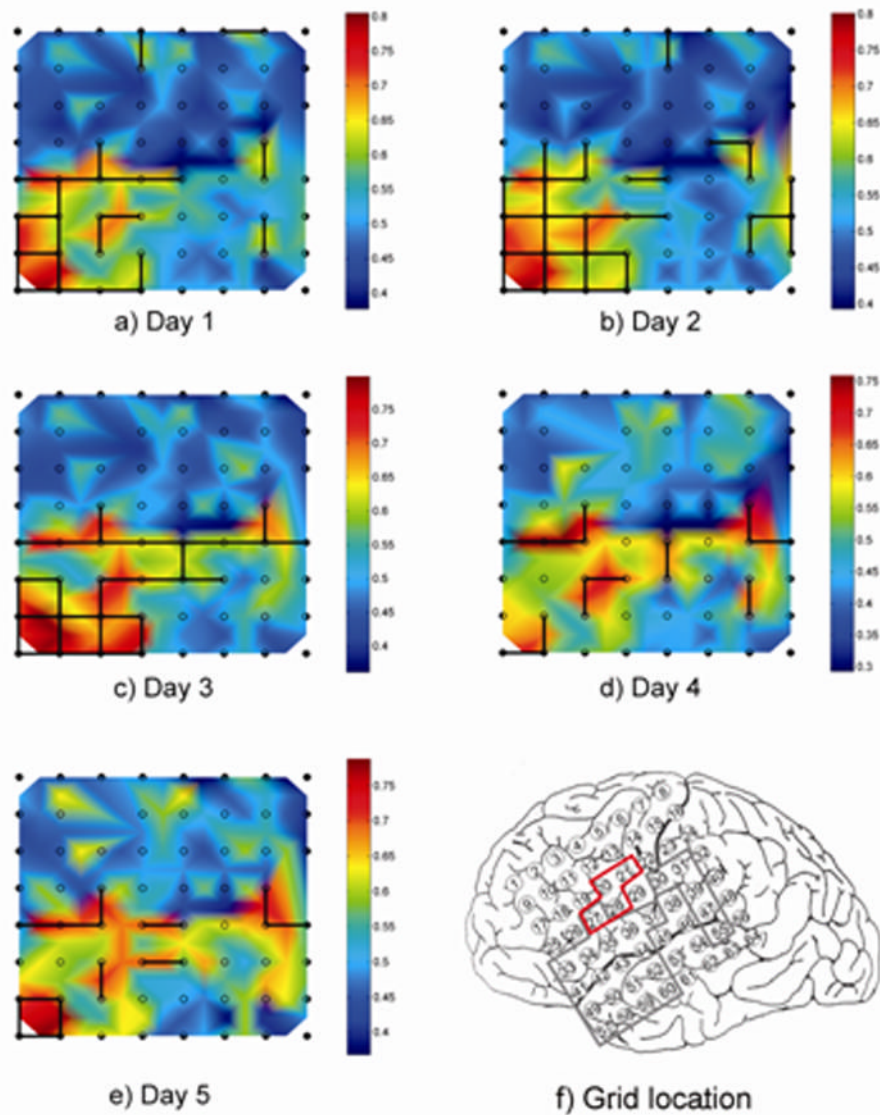


Figure 3. a–e) Daily snapshots of Patient 2’s 8×8 subdural grid, showing day to day variations in local synchrony and identification of LH channel pairs. The location of the grid on the cortical surface is shown in f), with electrode 1 corresponding to the top left corner of the grid maps and electrode 8 to the top right corner. Snapshots were selected from 125 time samples taken over a 5 day monitoring period. Two LH regions are seen, one in the anterior/inferior portion of the grid (frontal and temporal perisylvian region) and one more posteriorly in the parietal lobe. Day to day variations primarily occur at the boundaries of the LH regions, while the core areas are consistently identified as LH in each day’s recording; note that at one point the two regions appear to merge. The boundaries of the presumed epileptogenic zone and resection target area in the grid are indicated with the red tracing in f), while the locally hypersynchronous regions are shown traced in gray.

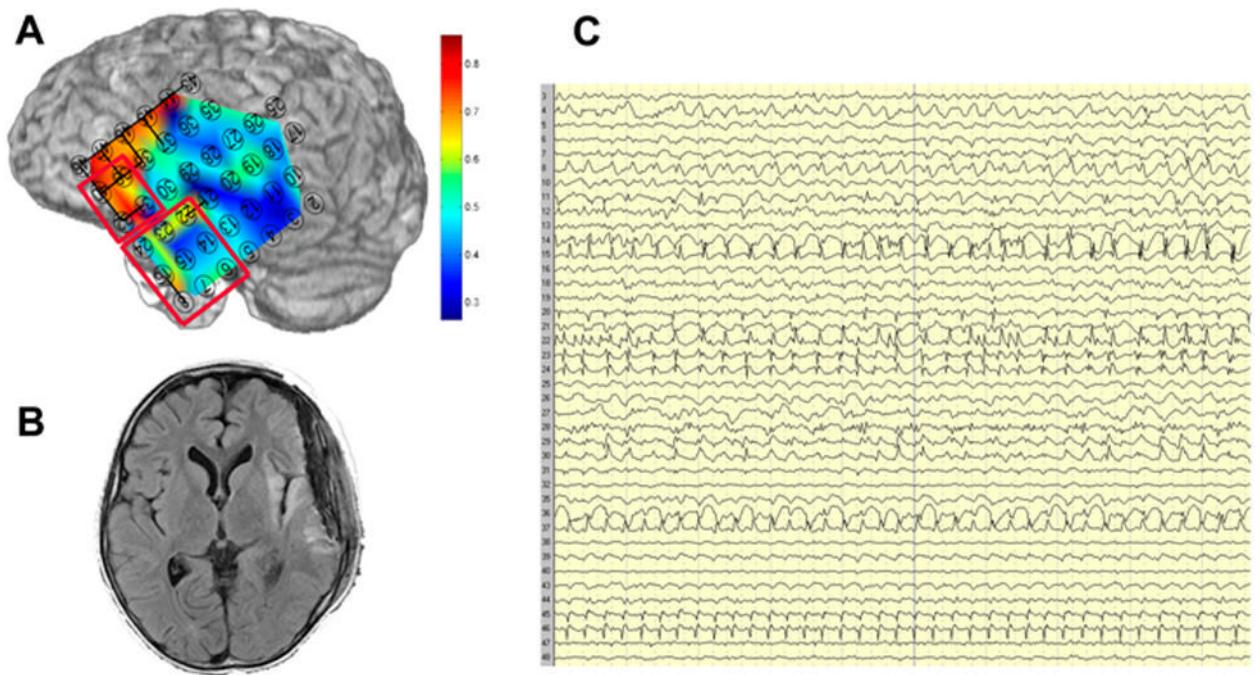


Figure 4. Spatial variation in local 5-minute average MPC in Patient 3, a 9 year old with Parry-Romberg syndrome and a left peri-insular lesion in prolonged focal status epilepticus. a) Marked local hypersynchrony in the inferior frontal region as compared to the lateral temporal region. The frontal and temporal resections are shown in red outline. b) T2-weighted image showing the perisylvian lesion. c) Intracranial EEG showing typical ictal activity broadly distributed across the left fronto-temporal grid. Compared to the synchrony map, the differences between the frontal and temporal regions are difficult to appreciate on visual inspection.

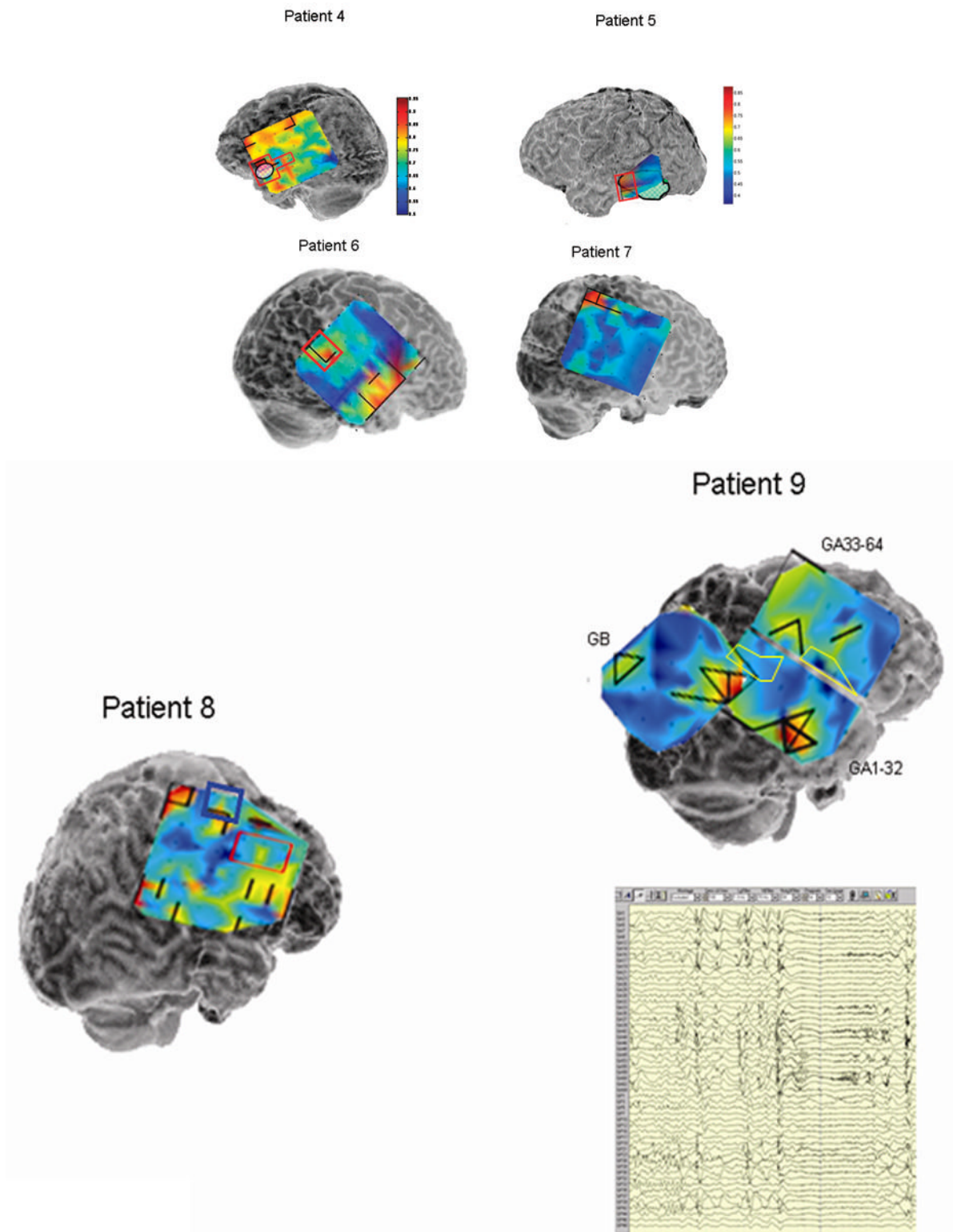


Figure 5. Local synchrony patterns and clinically identified epileptogenic zones (red boxes) in subdural grid recordings of Patients 4 – 9. The grid maps are as described in Figures 2 and 3. a) Local

hypersynchrony over well-defined structural lesions (Patients 4 and 5). The lesions are indicated by the hatched outlined areas. b) LH regions in the anterior temporal region (Patient 6) and parietal lobes (Patients 6 and 7). The red boxed area in Patient 6 was included in the resection, while no neocortical areas were resected in Patient 7. c) LH regions in nonlesional frontal lobe epilepsy (Patients 8 and 9). Note the relative locations of the LH regions and epileptogenic zones in Patient 8. Patient 9's LH regions indicated a surprising degree of focality given the widespread activity on the EEG. Based on the EEG findings, Patient 9 underwent two resections: lateral temporal lobe anterior to a language-critical area found on neurostimulation mapping, and a near-complete functional frontal lobectomy sparing primary motor and Broca's area. The language-critical areas are shown traced in yellow.

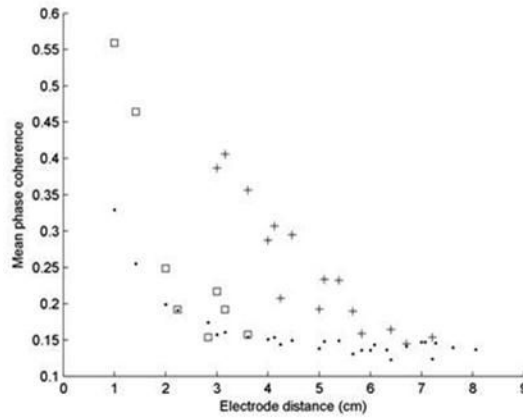


Figure 6.

Plots of the 5-minute average MPC vs. interelectrode distance for Patient 1. Solid dots denote channel pairs for which both electrodes were outside of LH areas. Squares denote electrode pairs belonging to a single LH region, while crosses denote electrode pairs located in noncontiguous LH regions. Note that local synchrony values are represented by the data at $x = 1$. The data show that LH electrode pairs nearly always had higher synchrony values than non-LH pairs regardless of the distance between them; the synchrony between the two LH regions (shown in Figure 2) is especially prominent.

Table 1

Subjects' clinical data

Subjects' clinical ICEEG data with location of LH regions

Pt #	Age	Age of seizure onset	Pathology	Implant Location	LH regions	Resection	Clinical Outcome
1	36	20	NC	Right temporo-occipital	Suprasylvian frontal, posterior temporal	Posterior temporal	No change
2	29	2	Perisylvian cortical dysplasia	Left central and temporal	Perisylvian (frontal and temporal)	Dorso-lateral frontal	No change
3	9	8	NC	Left frontotemporal	Inferior frontal	*Temporal and inferior frontal	Improved
4	54	12	Cavernous angioma	Left temporal	Anterior temporal	N/A	N/A
5	17	17	Glioma	Left temporal	Lateral temporal	Lesionectomy and additional topectomy anterior to tumor	Seizure-free
6	26	11	MTS	Right temporo-parietal	Anterior temporal, parietal	Standard nondominant temporal lobectomy, parietal topectomy	Seizure-free
7	26	22	MTS	Right temporo-parietal	Parietal	Standard nondominant temporal lobectomy	Improved; residual simple partial seizures
8	40	5	NC	Right frontotemporal	Frontal (multiple)	Anteroinferior frontal and supplementary motor	Improvement
9	42	13	NC	Broad right hemisphere	Frontal, anterior temporal, parietal	Frontal (sparing eloquent cortex), anterior temporal	Improvement

* Resection based on recording of status epilepticus

NC = no clear pathological diagnosis

MPC data description for the interictal samples tested (mean/std deviation, LH threshold, electrode pairs)

Characteristics of local synchrony distributions and identification of LH channels for the three interictal ICEEG samples recorded from each patient (Patient 2's data is shown separately in the text and in Figure 3). The distribution of the averaged MPC values per channel pair is described by the range, mean, standard deviation, and skew; as kurtosis was variable these data are not shown. The LH threshold, computed by the de-skewing algorithm described in the Methods section, and the number of resulting LH pairs are shown for each sample. The deviation of the MPC values computed from the second and third samples from the baseline, or first sample, is shown as the mean and standard deviation of the percentage change for each channel pair. The last column shows the number of electrodes identified as part of an LH pair in all three samples. These data show that, while some variation in the MPC values, LH threshold, and number of pairs are present between samples, there is a "core" set of electrodes that consistently identify cortical regions with the hypersynchrony property.

Pt #	Sample 1 MPC distribution			Sample 1 LH		Sample 2		Sample 3		Core Electrodes	
	Range	Mean, σ	Skew	Threshold	Pairs	%Change	Threshold	Pairs	%Change	Threshold	Pairs
1	0.15 – 0.74	0.37/0.19	0.62	0.52	8	11, 10	0.50	11	8, 6	0.54	9
3	0.26 – 0.86	0.51/0.14	0.54	0.62	15	4, 3	0.62	17	3, 2	0.59	20
4	0.26 – 0.70	0.45/0.10	0.50	0.56	19	11, 8	0.60	9	7, 6	0.62	10
5	0.20 – 0.88	0.50/0.20	1.19	0.63	4	4, 2	0.59	4	2, 1	0.60	4
6	0.23 – 0.99	0.49/0.15	0.65	0.66	12	4, 3	0.67	12	2, 2	0.68	10
7	0.36 – 0.66	0.51/0.06	0.42	0.59	5	6, 5	0.62	2	8, 12	0.62	2
8	0.29 – 0.72	0.49/0.09	0.44	0.61	10	12, 9	0.56	29	9, 8	0.67	6
9	0.30 – 0.67	0.43/0.07	0.50	0.54	6	10, 6	0.59	3	5, 4	0.51	7

** Calculations are for fronto-temporal grid with a distance of 2cm due to sampling of grid electrodes; parietal grid was analyzed separately.